IEEE Access
Multidisciplinary | Rapid Review | Open Access Journal

Received June 18, 2018, accepted August 19, 2018, date of publication August 27, 2018, date of current version September 21, 2018.

Digital Object Identifier 10.1109/ACCESS.2018.2866910

Performance Analysis of Wireless Powered Incremental Relaying Networks With an Adaptive Harvest-Store-Use Strategy

GUOXIN LI AND HAI JIANG, (Senior Member, IEEE)
Department of Electrical and Computer Engineering, University of Alberta, Edmonton, AB T6G 1H9, Canada
Corresponding author: Hai Jiang (hai1@ualberta.ca)

This work was supported in part by the Alberta Innovates Graduate Student Scholarship and in part by the Natural Sciences and Engineering Research Council of Canada.

ABSTRACT In this paper, we consider a wireless powered cooperative network, in which a source with constant power supply communicates with a destination under the assistance of an energy harvesting (EH) relay. From signals of the source, the relay can perform EH and information decoding simultaneously by using the power splitting (PS) technique. To increase the spectrum efficiency of the system and save energy consumption at the relay, an incremental decode-and-forward (IDF) relaying protocol is adopted to forward information. Inspired by the features of the IDF protocol, we propose a new energy harvesting and use strategy, named adaptive harvest-store-use (AHSU). In this proposed strategy, the relay adaptively sets its PS ratio according to a one-bit feedback from the destination, the channel estimation result for the source-to-relay link, and the relay's energy status. A finite-state Markov chain (MC) is employed to model the charging/discharging behavior of the relay's battery. The steady-state distribution of the MC is first derived, and then used to calculate the exact outage probability. In order to gain further insights, we investigate the outage performance of the system when the transmit signal-to-noise ratio of the source is high. Based on the asymptotic outage probability expression, the diversity order and coding gain are characterized, which demonstrates that a full diversity order is achieved by our proposed AHSU strategy in the considered network.

INDEX TERMS Energy harvesting, diversity order, incremental relaying, power splitting, relays, wireless communication.

I. INTRODUCTION

With the rapid growth of communication networks, the communications industry is taking more and more share of energy consumption. How to improve energy efficiency in the next generation communication network has become a key issue [1]. Energy harvesting (EH), which extracts energy from the environment, has been viewed as a promising technique to solve the problem [2]–[4]. Compared to natural renewable energy sources (e.g., tidal, solar, and wind), which are unstable and random, harvesting energy from man-made radio frequency (RF) signals is more appealing since RF signals are controllable and can carry information and energy simultaneously [5]–[8]. The technique of simultaneous wireless information and power transfer (SWIPT) has been extensively studied in different types of communication networks [9]–[13]. In particular, cooperative SWIPT network is one of the important application scenarios.

It is known that incorporating the relaying technique into a point-to-point network efficiently extends communication coverage by exploiting spatial diversity. But this promising advantage is realized at the cost of additional energy consumption at the relay nodes, which may prevent those energy-constrained nodes from serving as relays. To encourage energy-constrained nodes to participate in the information forwarding, SWIPT technique is introduced to traditional relay networks, in which the relays extract energy from the source's signals, and then use the harvested energy for information forwarding. Based on these observations, wireless powered[1] cooperative networks (WPCNs) with SWIPT have drawn considerable attentions recently. In accordance with the two practical EH receiver architectures that are

[1]Note that, the terms ''wireless powered'' and ''energy harvesting'' are used interchangeably in this paper.

proposed in a point-to-point SWIPT system [9], namely power splitting (PS) and time switching (TS), the work in [13] correspondingly proposes two protocols for WPCNs to achieve SWIPT: PS-based relaying (PSR) and TS-based relaying (TSR).

Most of current works on WPCNs assume that a relay either uses up the harvested energy in the subsequent forwarding phase or discards the harvested energy if it is not selected to forward information, which is referred to as the harvest-use (HU) strategy. Obviously, this strategy under-utilizes the harvested energy. If the relay has the energy storage capability and can adaptively adjust its energy harvesting and use strategy according to the channel conditions, system performance is expected to further improve [14], [15]. Inspired by this, some initial efforts have been put on the study of WPCNs, in which the relay can harvest and store energy [16]–[22]. The work in [16] proposes to use a discretized Markov chain (MC) to model the charging and discharging behavior of an EH-based relay in a classical three-node WPCN network. This work is later extended to multi-relay scenarios in [17]–[21]. Assuming that relays are clustered together, two different single relay selection schemes are proposed in [17] and [18], respectively. In [17], one of the relays in the successful decoding set which has the best relay-destination link is chosen to forward information. However, the relay that has the best relay-destination link might not have enough power to forward information. Seeing this issue, the work in [18] proposes a robust relay selection scheme which takes into consideration both the channel state information (CSI) and the energy state of relays. The work in [19] develops a distributed and energy based multi-relay selection scheme, and shows that the outage performance and packet error performance can be improved by the proposed scheme. In the case of random distribution of relay locations, several relay selection schemes are proposed in [20] to achieve a good tradeoff between performance and implementation complexity. One common assumption in [16]–[20] is that a relay cannot perform EH and information processing (IP) simultaneously, i.e., the received signal at the relay is totally allocated to the IP circuit or the EH circuit. This setting inefficiently utilizes the received signal power since the relay may only need a portion of the source's signal for IP (e.g., for decoding information of the source), while the remaining portion of the source's signal can be used for EH. If the PS protocol is adopted, the relay is actually able to perform EH and IP simultaneously. The work in [21] investigates the throughput maximization problems for the WPCNs with PSR protocol when different CSI is provided.

Different from [16]–[21] that the direct link from the source to the destination is ignored, in this paper we study a three-node WPCN with the direct link taken into consideration. It is known [23]–[25] that the existence of a direct link from the source to the destination can improve the performance of the cooperative network by providing a diversity gain and a multiplexing gain. Generally, the direct link's channel may fluctuate due to fading. If the direct link does not have a good channel gain to support the transmission to the destination, the relay can be requested to participate in cooperation that consists of two phases: the source transmits in the first phase, while the relay forwards in the second phase. When the direct link has a good channel gain to support the transmission to the destination, it is better to use the direct link only, because 1) the source can transmit in both phases, and 2) the relay can perform EH during the two phases and store the harvested energy in its battery (which means that the relay can accumulate more energy, and thus, it can have a higher transmit power in later time when the direct link is weak and the cooperation of the relay is requested). This observation motivates us to find an adaptive energy harvesting and use strategy which takes both the status of the direct link and the relay link (source-relay-destination) into consideration. To the best of our knowledge, there is very limited work in the literature that involves this issue. By using the incremental relaying (IR) protocol introduced in [26], the work in [22] proposes a heuristic incremental accumulate-then-forward (IATF) relaying protocol for an EH-based relay network with a direct link. More specifically, in IR, the destination sends one-bit feedback to indicate whether the relay's assistance is requested. Owing to this feature of IR, the IATF protocol enables the relay to have more chances to harvest and accumulate energy when the direct link is in good condition. However, the IATF protocol suggests that in the first time slot,[2] the relay should decode message as long as its residual energy is larger than a predefined energy threshold. This design wastes the opportunity to harvest energy when the direct link suffers no outage. In addition, the relay in IATF cannot work in the EH and IP modes simultaneously. To address these two issues, we propose a new energy harvesting and use strategy, named adaptive harvest-store-use (AHSU), for a three-node WPCN. Our main contributions are summarized as follows:

- We consider a WPCN with a direct link taken into account. Specifically, a PS-based relay that adopts an IR protocol can harvest energy and decode information simultaneously. Inspired by the features of the IR protocol, we propose the AHSU strategy in which the relay is allowed to adaptively adjust its PS ratio according to a one-bit feedback from the destination, the relay's channel estimation result for the source-to-relay link, and the relay's energy status.
- To facilitate performance evaluation, we employ a finite-state MC to model the state evolution of the relay's battery. The state transition matrix of the MC is firstly developed, based on which we then derive the exact steady-state distribution of the MC, and finally obtain the desired exact outage probability expression.
- To provide further insights for practical system design, asymptotic outage performance of the considered

[2]For the IATF transmission protocol, each transmission block consists of two time slots.

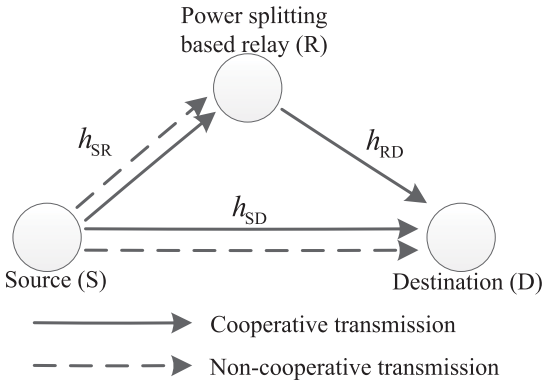

FIGURE 1. The considered three-node cooperative network.

system is also studied. First, we derive an approximated steady-state distribution of the MC in the high signal-to-noise ratio (SNR) regime. Then a simple asymptotic outage probability expression is obtained, which illustrates that the considered system with our proposed AHSU strategy can achieve a full diversity order.

In our work, we use a finite-state MC model similar to that in [16], to model the state evolution of the relay's battery. The differences between our work and the work in [16] are as follows. 1) The work in [16] assumes that no direct link exists between the source and destination, while we assume a direct link between the source and destination, and we use an IR protocol. 2) The work in [16] assumes that the relay has perfect knowledge of the instantaneous CSI of its link to the destination. In our work, we do not assume this knowledge, to save communication overhead. 3) The work in [16] assumes that the relay cannot perform EH and IP simultaneously. In our work, by using the PS protocol, the relay is able to perform EH and IP simultaneously.

The remainder of this paper is organized as follows. Section II presents the system model as well as the proposed AHSU strategy. Section III studies the exact and asymptotic outage performance of the considered system with the proposed AHSU strategy. Section IV provides numerical results to facilitate performance evaluation and comparison. Finally, Section V concludes this paper.

II. SYSTEM MODEL

We consider a classical three-node cooperative network shown in Fig. 1, where a source (S) with a constant power supply communicates with a destination (D) under the assistance of a PS-based EH relay (R). As depicted in Fig. 2, R adopts the PS technique to decode information and harvest energy simultaneously, and the harvested energy is then stored in R's battery before being used to transmit information. Each node works in the half-duplex mode and has a single antenna. All the links (S $\rightarrow$ D, S $\rightarrow$ R, and R $\rightarrow$ D) experience both

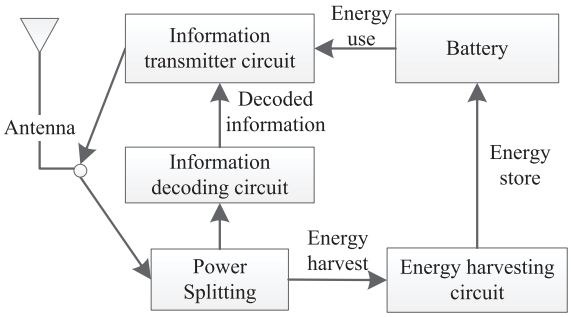

FIGURE 2. Architecture of the relay.

Rayleigh fading and path-loss effects.[3] The channel coefficient h_{XY} for the $X \rightarrow Y$ link follows a complex Gaussian distribution with zero mean and variance $\Omega_{XY} = \lambda d_{XY}^{-\nu}$, where $(X, Y) \in \{(\mathrm{S,R}), (\mathrm{R,D}), (\mathrm{S,D})\}$, λ denotes the path gain corresponding to a distance of 1 meter, d_{XY} is the distance between X and Y, and ν is the path-loss exponent [27]. In addition, we assume that h_{XY} remains unchanged within one transmission block with duration T, but varies independently from one block to the next. The received signal at each node is corrupted by additive white Gaussian noise (AWGN) with zero mean and variance σ^2. Moreover, considering that R is energy constrained, we assume that only the receiver side in the network can perfectly access local CSI, which can reduce the overhead involved in CSI acquisition.

A. ADAPTIVE HARVEST-STORE-USE STRATEGY

Consider a target transmission block with duration T, which is divided into two time slots, each with duration $T/2$. Before describing our proposed AHSU strategy, we would like to first introduce the battery model of R. R is equipped with a rechargeable battery with the size $E_{\mathrm{R}} = \varpi E_0$, where $E_0 \triangleq \frac{P_{\mathrm{S}} T}{2}$, P_{S} is the transmit power of S, and $\varpi > 0$. At any moment, the battery level is a continuous value, which makes analysis difficult. To facilitate analysis, an $(N+1)$-level uniform quantization model is employed to deal with the battery energy state. Specifically, the battery capacity E_{R} is uniformly quantized in units of energy quantum $E_u \triangleq \delta E_0$, where $\delta \triangleq \frac{\varpi}{N}$, and thus, we have $(N+1)$ energy states $\{0, E_u, ..., NE_u\}$. Moreover, let $E_{\mathrm{ini}} \triangleq iE_u$, $0 \leq i \leq N$, denote the energy level in R's battery at the beginning of the target transmission block.

[3] For mathematical tractability to provide insights on the proposed AHSU strategy, we assume that all the links' fading are Rayleigh fading. This is an assumption that has been adopted by many other works [13]–[18], [20], [21], [23]–[25]. In real networks, it is likely that some link(s) may follow different fading. If such a more general case is considered, our derivations in equations (1)–(27) are still valid after replacing functions $F_{|\cdot|^2}(\cdot)$ and $\bar{F}_{|\cdot|^2}(\cdot)$ in those equations by the cumulative distribution function and complementary cumulative distribution function, respectively, for the corresponding fading models. In the asymptotic outage performance analysis in equations (28)–(32), the derivations are based on the fact that the channel gain of a Rayleigh fading link follows exponential distribution, and thus, the derivations may not be valid for other fading models (for example, Rician and Nakagami-m). We leave asymptotic outage performance analysis with other fading models for future investigation.

The proposed AHSU strategy, which is based on an incremental decode-and-forward (IDF) protocol, includes three parts: energy harvest, energy store, and energy use. In general, in a transmission block, when the direct link is good enough to support the target information rate from S to D, then R works in the non-cooperative mode: during the two time slots in the transmission block, R only *harvests* energy (i.e., without information decoding) and *stores* the harvested energy in its battery. When the direct link is not good enough and cooperation of R is requested, R decides whether to be in the cooperative mode or the non-cooperative mode based on its local estimation of $|h_{\rm SR}|^2$ and its energy status. If R decides to be in the non-cooperative mode, then during the first time slot, it only *harvests* energy (i.e., without information decoding) and *stores* the harvested energy in its battery, and during the second time slot it keeps silent. If R decides to be in the cooperative mode, then during the first time slot it uses PS to decode information and *harvest* energy simultaneously, and *stores* the harvested energy in its battery, and in the second time slot it *uses* all the energy in its battery to forward information to D. The details are given in the following.

At the beginning of the first time slot, S first broadcasts a pilot signal to R and D. D performs channel estimation based on the received pilot signal. If $|h_{\rm SD}|^2 \geq \frac{\gamma_{\rm th}}{\rho_0}$ ($\rho_0 = P_{\rm S}/\sigma^2$ is the transmit SNR, $\gamma_{\rm th} = 2^{R_t} - 1$, R_t is the target information rate of S to D), D can decode S's message directly, and thus, it feeds back a one-bit positive acknowledgment (ACK) to S and R. If $|h_{\rm SD}|^2 < \frac{\gamma_{\rm th}}{\rho_0}$, D feeds back a one-bit negative acknowledgment (NACK) to S and R.

If D feeds back an ACK, S sends information with rate R_t in the two time slots of the target transmission block. And R works in the non-cooperative mode by only harvesting energy and storing energy during the two time slots.

If D feeds back an NACK, S sends information with rate $2R_t$ in the first time slot, and keeps silent in the second time slot (as S expects R to transmit in the second time slot). Based on the estimated channel gain $|h_{\rm SR}|^2$, R decides whether it is able to decode the received signal from S in the first time slot.

- If R can decode S's message in the first time slot (i.e., $|h_{\rm SR}|^2$ is larger than $\frac{\gamma'_{\rm th}}{\rho_0}$ in which $\gamma'_{\rm th} = 2^{2R_t} - 1$) and R can have at least one energy quantum E_u for forwarding,[4] then R works in the cooperative mode as follows. In the first time slot, R performs information decoding and EH by using the PS technique, and stores the harvested energy in its battery. Since R has no CSI of S $\rightarrow$ D or R $\rightarrow$ D link, R uses up (best-effort transmission) the stored energy in its battery to forward the re-coded information in the second time slot, and D combines the received signals from S and R in the first and second time slots, respectively, with the maximal ratio combining (MRC) technique.
- If R cannot decode S's message in the first time slot (i.e., $|h_{\rm SR}|^2$ is smaller than $\frac{\gamma'_{\rm th}}{\rho_0}$), or R is unable to have at least one energy quantum E_u for forwarding, then R works in the non-cooperative mode, i.e., it only harvests energy and stores the harvested energy in its battery in the first time slot, and keeps silent in the second time slot (as S does not transmit in the second time slot).[5]

Modeling of the three parts (energy harvest, energy store, and energy use) of the AHSU strategy is given below.

1) ENERGY HARVEST

Denote by θ the PS ratio, which indicates that θ proportion of the received signal power at R is used for EH and the remaining part is used for information decoding. R adaptively sets its PS ratio according to the 1-bit feedback from D, the channel estimation result of $|h_{\rm SR}|^2$, and its energy status, which can be classified as the following three cases:

Case 1: When R gets the ACK transmitted by D, R sets θ to 1 in the two time slots, which means that all the received power at R is allocated to the EH device. This setting is intuitive since R should not waste any received power on information decoding if it does not need to forward information. Thus, the final harvested energy within the target transmission block can be written as

$$E_h = \eta P_{\rm S} |h_{\rm SR}|^2 T = 2\eta |h_{\rm SR}|^2 E_0, \tag{1}$$

where $0 < \eta < 1$ is the energy conversion efficiency.

Case 2: D feedbacks an NACK requesting R's assistance, and R has residue energy, i.e., $E_{\rm ini} > 0$. Based on the channel estimation of $|h_{\rm SR}|^2$, R judges whether or not it can decode S's message successfully. If it can decode, i.e., $|h_{\rm SR}|^2 \geq \frac{\gamma'_{\rm th}}{\rho_0}$, the PS ratio $\theta = 1 - \frac{\gamma'_{\rm th}}{\rho_0 |h_{\rm SR}|^2}$ is set, which can maximize the harvested energy while ensuring correct decoding [14]; otherwise R gives up decoding and directs the received signal to the EH device, i.e., $\theta = 1$. In this case, the harvested energy within the target transmission block can be expressed as

$$E_h = \begin{cases} \eta \left(|h_{\rm SR}|^2 - \frac{\gamma'_{\rm th}}{\rho_0} \right) E_0, & |h_{\rm SR}|^2 \geq \frac{\gamma'_{\rm th}}{\rho_0}, \\ \eta |h_{\rm SR}|^2 E_0, & |h_{\rm SR}|^2 < \frac{\gamma'_{\rm th}}{\rho_0}. \end{cases} \tag{2}$$

Case 3: D feedbacks an NACK but there is no energy left in R's battery, i.e., $E_{\rm ini} = 0$. If R wants to forward information in this case, R needs to ensure that at least one energy quantum E_u is collected besides the correct decoding, i.e., $\eta \left(|h_{\rm SR}|^2 - \frac{\gamma'_{\rm th}}{\rho_0} \right) E_0 \geq E_u$. Accordingly, if $|h_{\rm SR}|^2 \geq \frac{\gamma'_{\rm th}}{\rho_0} + \frac{\delta}{\eta}$, R sets the PS ratio to $\theta = 1 - \frac{\gamma'_{\rm th}}{\rho_0 |h_{\rm SR}|^2}$; otherwise the received signal is used only for EH with $\theta = 1$. The harvested energy within the target transmission block in this case is given by

$$E_h = \begin{cases} \eta \left(|h_{\rm SR}|^2 - \frac{\gamma'_{\rm th}}{\rho_0} \right) E_0, & |h_{\rm SR}|^2 \geq \frac{\gamma'_{\rm th}}{\rho_0} + \frac{\delta}{\eta}, \\ \eta |h_{\rm SR}|^2 E_0, & |h_{\rm SR}|^2 < \frac{\gamma'_{\rm th}}{\rho_0} + \frac{\delta}{\eta}. \end{cases} \tag{3}$$

[4] This means that R has at least one energy quantum E_u in its battery at the beginning of the transmission block, or can harvest at least one energy quantum E_u during the first time slot of the transmission block.

[5] Different from the IATF strategy in [22], S does not retransmit information in the second time slot in our work, for the following reason. When D feeds back an NACK (i.e., when $|h_{\rm SD}|^2 < \frac{\gamma_{\rm th}}{\rho_0}$), D should still fail to decode the information with the two pieces of the same information if S retransmits in the second time slot.

To this end, the PS ratio setting can be concluded as (4), as shown at the bottom of this page. Note that the value of θ also represents the forwarding strategy of R. $\theta = 1$ indicates that R works in the non-cooperative mode and harvests energy only, and $\theta = 1 - \frac{\gamma'_{\rm th}}{\rho_0 |h_{\rm SR}|^2}$ indicates that R works in the cooperative mode with the best effort transmission policy.

2) ENERGY STORE

The harvested energy is buffered in the battery before used for data transmission. As the quantized battery model is used and the battery capacity is limited, the final quantity of the harvested energy that can be stored in the battery is given by $\tilde{E}_h = lE_u$, where

$$l = \min\left\{\left\lfloor \frac{E_h}{E_u} \right\rfloor, N\text{-}i\right\} \tag{5}$$

in which $\lfloor\cdot\rfloor$ is a floor function, and $i \triangleq \frac{E_{\rm ini}}{E_u}$ as we have defined at the beginning of Section II-A. As such, the energy level in the battery after EH can be expressed as $\tilde{E}_h + E_{\rm ini}$.

3) ENERGY USE

According to the best-effort transmission policy, R exhausts the energy stored in the battery if it works in the cooperative mode; otherwise R keeps silent and does not consume energy.[6] Thus, the consumed energy of R within the target transmission block can be expressed as

$$E_c = \begin{cases} \tilde{E}_h + E_{\rm ini}, & \text{R in the cooperative mode,} \\ 0, & \text{R in the non-cooperative mode.} \end{cases} \tag{6}$$

B. BATTERY STATE TRANSITION

Let $E_{\rm end} \triangleq jE_u$, $0 \le j \le N$, denote the energy level in the battery at the end of the target transmission block. According to the AHSU strategy, the relationship between $E_{\rm ini}$ and $E_{\rm end}$ can be formulated as

$$\begin{aligned} E_{\rm end} &= E_{\rm ini} + \tilde{E}_h - E_c \\ &= \begin{cases} 0, & \text{R in the cooperative mode,} \\ \tilde{E}_h + E_{\rm ini}, & \text{R in the non-cooperative mode.} \end{cases} \end{aligned} \tag{7}$$

Similar to [16]–[21], we employ an $(N+1)$-state MC to model the battery energy state transition, where state s_k $(0 \le k \le N)$ represents that the energy level in the battery is equal to kE_u. Recall that $E_{\rm ini} \triangleq iE_u$ and $E_{\rm end} \triangleq jE_u$, which means that the relay's battery is at state s_i at the beginning of the target transmission block, and is at state s_j at the end of the transmission block. Next, we determine the transition probability matrix of the MC, i.e., $\mathbf{P} = \left[P_{i,j}\right]_{(N+1)\times(N+1)}$, where $P_{i,j}$ denotes the one-step transition probability from state s_i to s_j.

1) $s_0 \to s_0$

The empty state remains unchanged in the following two cases: i) R lies in the non-cooperative mode, while the harvested energy E_h is less than one energy quantum E_u; ii) R enters the cooperative mode, and uses up the energy stored in the battery to forward information. Accordingly, the transition probability of $s_0 \to s_0$ can be evaluated as

$$\begin{aligned} P_{0,0} = &\underbrace{\Pr\{E_h < E_u, \theta = 1 | E_{\rm ini} = 0\}}_{P'_{0,0}} \\ &+ \underbrace{\Pr\left\{\theta = 1 - \frac{\gamma'_{\rm th}}{\rho_0 |h_{\rm SR}|^2} | E_{\rm ini} = 0\right\}}_{P''_{0,0}}, \end{aligned} \tag{8}$$

in which $\Pr\{\cdot\}$ means probability.

$P'_{0,0}$ and $P''_{0,0}$ in (8) are respectively calculated as

$$\begin{aligned} &P'_{0,0} \\ &= \Pr\left\{|h_{\rm SD}|^2 \ge \frac{\gamma_{\rm th}}{\rho_0}, 2\eta|h_{\rm SR}|^2 E_0 < \delta E_0\right\} \\ &\quad + \Pr\left\{|h_{\rm SD}|^2 < \frac{\gamma_{\rm th}}{\rho_0}, |h_{\rm SR}|^2 < \frac{\gamma'_{\rm th}}{\rho_0} + \frac{\delta}{\eta}, \eta|h_{\rm SR}|^2 E_0 < \delta E_0\right\} \\ &= \bar{F}_{|h_{\rm SD}|^2}\left(\frac{\gamma_{\rm th}}{\rho_0}\right) F_{|h_{\rm SR}|^2}\left(\frac{\delta}{2\eta}\right) + F_{|h_{\rm SD}|^2}\left(\frac{\gamma_{\rm th}}{\rho_0}\right) F_{|h_{\rm SR}|^2}\left(\frac{\delta}{\eta}\right), \end{aligned} \tag{9}$$

and

$$\begin{aligned} P''_{0,0} &= \Pr\left\{|h_{\rm SD}|^2 < \frac{\gamma_{\rm th}}{\rho_0}, |h_{\rm SR}|^2 \ge \frac{\gamma'_{\rm th}}{\rho_0} + \frac{\delta}{\eta}\right\} \\ &= F_{|h_{\rm SD}|^2}\left(\frac{\gamma_{\rm th}}{\rho_0}\right) \bar{F}_{|h_{\rm SR}|^2}\left(\frac{\gamma'_{\rm th}}{\rho_0} + \frac{\delta}{\eta}\right), \end{aligned} \tag{10}$$

where $F_{|h_{XY}|^2}(x) = 1 - e^{-\frac{x}{\Omega_{XY}}}$ and $\bar{F}_{|h_{XY}|^2}(x) = e^{-\frac{x}{\Omega_{XY}}}$ denote the cumulative distribution function (CDF) and the complementary cumulative distribution function (CCDF) of the exponential random variable $|h_{XY}|^2$, respectively, and $(X, Y) \in \{(\text{S,R}), (\text{R,D}), (\text{S,D})\}$.

2) $s_i \to s_j (0 \le i < j < N)$

The non-full battery can be partially charged when R stays in the non-cooperative mode, while E_h is larger than $(j-i)E_u$ but smaller than $(j-i+1)E_u$. The transition probability of this case can be expressed as (11), as shown at the bottom of the next page, where $A_{i,j}$, $B_{i,j}$ and $C_{i,j}$ $(0 \le i < j < N)$ are

[6] In accordance with most of current works, we also assume that the circuit power consumption at R can be neglected. Our research can be straightforwardly extended to the case when a fixed circuit power consumption is taken into account.

$$\theta = \begin{cases} 1 - \frac{\gamma'_{\rm th}}{\rho_0 |h_{\rm SR}|^2}, & \left(|h_{\rm SD}|^2 < \frac{\gamma_{\rm th}}{\rho_0}\right) \cap \left\{\left(|h_{\rm SR}|^2 \ge \frac{\gamma'_{\rm th}}{\rho_0} + \frac{\delta}{\eta} | E_{\rm ini} = 0\right) \cup \left(|h_{\rm SR}|^2 \ge \frac{\gamma'_{\rm th}}{\rho_0} | E_{\rm ini} > 0\right)\right\}, \\ 1, & \left(|h_{\rm SD}|^2 \ge \frac{\gamma_{\rm th}}{\rho_0}\right) \cup \left(|h_{\rm SR}|^2 < \frac{\gamma'_{\rm th}}{\rho_0} + \frac{\delta}{\eta} | E_{\rm ini} = 0\right) \cup \left(|h_{\rm SR}|^2 < \frac{\gamma'_{\rm th}}{\rho_0} | E_{\rm ini} > 0\right). \end{cases} \tag{4}$$

respectively given by

$$A_{i,j} = \bar{F}_{|h_{\mathrm{SD}}|^2}\left(\frac{\gamma_{\mathrm{th}}}{\rho_0}\right) \times \left[F_{|h_{\mathrm{SR}}|^2}\left(\frac{(j-i+1)\,\delta}{2\eta}\right) - F_{|h_{\mathrm{SR}}|^2}\left(\frac{(j-i)\,\delta}{2\eta}\right)\right], \quad (12)$$

$$B_{i,j} = \begin{cases} 0, & \frac{\gamma'_{\mathrm{th}}}{\rho_0} < \frac{(j-1)\delta}{\eta}, \\ \left[F_{|h_{\mathrm{SR}}|^2}\left(\frac{\gamma'_{\mathrm{th}}}{\rho_0} + \frac{\delta}{\eta}\right) - F_{|h_{\mathrm{SR}}|^2}\left(\frac{j\delta}{\eta}\right)\right] & \\ \times F_{|h_{\mathrm{SD}}|^2}\left(\frac{\gamma_{\mathrm{th}}}{\rho_0}\right), & \frac{(j-1)\delta}{\eta} \le \frac{\gamma'_{\mathrm{th}}}{\rho_0} < \frac{j\delta}{\eta}, \\ \left[F_{|h_{\mathrm{SR}}|^2}\left(\frac{(j+1)\delta}{\eta}\right) - F_{|h_{\mathrm{SR}}|^2}\left(\frac{j\delta}{\eta}\right)\right] & \\ \times F_{|h_{\mathrm{SD}}|^2}\left(\frac{\gamma_{\mathrm{th}}}{\rho_0}\right), & \frac{\gamma'_{\mathrm{th}}}{\rho_0} \ge \frac{j\delta}{\eta}, \end{cases} \quad (13)$$

and

$$C_{i,j} = \begin{cases} 0, & \frac{\gamma'_{\mathrm{th}}}{\rho_0} < \frac{(j-i)\,\delta}{\eta}, \\ \left[F_{|h_{\mathrm{SR}}|^2}\left(\frac{\gamma'_{\mathrm{th}}}{\rho_0}\right) - F_{|h_{\mathrm{SR}}|^2}\left(\frac{(j-i)\,\delta}{\eta}\right)\right] & \\ \times F_{|h_{\mathrm{SD}}|^2}\left(\frac{\gamma_{\mathrm{th}}}{\rho_0}\right), & \frac{(j-i)\,\delta}{\eta} \le \frac{\gamma'_{\mathrm{th}}}{\rho_0} < \frac{(j-i+1)\,\delta}{\eta}, \\ \left[F_{|h_{\mathrm{SR}}|^2}\left(\frac{(j-i+1)\delta}{\eta}\right) - F_{|h_{\mathrm{SR}}|^2}\left(\frac{(j-i)\,\delta}{\eta}\right)\right] & \\ \times F_{|h_{\mathrm{SD}}|^2}\left(\frac{\gamma_{\mathrm{th}}}{\rho_0}\right), & \frac{\gamma'_{\mathrm{th}}}{\rho_0} \ge \frac{(j-i+1)\,\delta}{\eta}. \end{cases} \quad (14)$$

3) $s_i \to s_N (0 \le i < N)$

The non-full battery can be fully charged when R lies in the non-cooperative mode, and E_h is no less than $(N-i)\,E_u$. Accordingly, the transition probability for this case can be formulated as (15), as shown at the bottom of this page, where $A_{i,N}$, $B_{i,N}$ and $C_{i,N}$ $(0 \le i < N)$ are respectively given by

$$A_{i,N} = \bar{F}_{|h_{\mathrm{SD}}|^2}\left(\frac{\gamma_{\mathrm{th}}}{\rho_0}\right)\bar{F}_{|h_{\mathrm{SR}}|^2}\left(\frac{(N-i)\,\delta}{2\eta}\right), \quad (16)$$

$$B_{i,N} = \begin{cases} 0, & \frac{\gamma'_{\mathrm{th}}}{\rho_0} < \frac{(N-1)\delta}{\eta}, \\ \left[F_{|h_{\mathrm{SR}}|^2}\left(\frac{\gamma'_{\mathrm{th}}}{\rho_0} + \frac{\delta}{\eta}\right) - F_{|h_{\mathrm{SR}}|^2}\left(\frac{\varpi}{\eta}\right)\right] & \\ \times F_{|h_{\mathrm{SD}}|^2}\left(\frac{\gamma_{\mathrm{th}}}{\rho_0}\right), & \frac{\gamma'_{\mathrm{th}}}{\rho_0} \ge \frac{(N-1)\delta}{\eta}, \end{cases} \quad (17)$$

and

$$C_{i,N} = \begin{cases} 0, & \frac{\gamma'_{\mathrm{th}}}{\rho_0} < \frac{(N-i)\,\delta}{\eta}, \\ \left[F_{|h_{\mathrm{SR}}|^2}\left(\frac{\gamma'_{\mathrm{th}}}{\rho_0}\right) - F_{|h_{\mathrm{SR}}|^2}\left(\frac{(N-i)\,\delta}{\eta}\right)\right] & \\ \times F_{|h_{\mathrm{SD}}|^2}\left(\frac{\gamma_{\mathrm{th}}}{\rho_0}\right), & \frac{\gamma'_{\mathrm{th}}}{\rho_0} \ge \frac{(N-i)\,\delta}{\eta}. \end{cases} \quad (18)$$

4) $s_i \to s_i (1 \le i \le N-1)$

The battery remains in a non-empty and non-full state when R stays in the non-cooperative mode while E_h is less than the

$$\begin{aligned} P_{i,j} &= \Pr\{\theta = 1, (j-i)\,E_u \le E_h < (j-i+1)\,E_u\} \\ &= \underbrace{\Pr\left\{|h_{\mathrm{SD}}|^2 \ge \frac{\gamma_{\mathrm{th}}}{\rho_0}, (j-i)\,\delta E_0 \le 2\eta|h_{\mathrm{SR}}|^2 E_0 < (j-i+1)\,\delta E_0\right\}}_{A_{i,j}} \\ &\quad + \begin{cases} \underbrace{\Pr\left\{|h_{\mathrm{SD}}|^2 < \frac{\gamma_{\mathrm{th}}}{\rho_0}, |h_{\mathrm{SR}}|^2 < \frac{\gamma'_{\mathrm{th}}}{\rho_0} + \frac{\delta}{\eta}, (j-i)\,\delta E_0 \le \eta|h_{\mathrm{SR}}|^2 E_0 < (j-i+1)\,\delta E_0\right\}}_{B_{i,j}}, & i = 0, \\ \underbrace{\Pr\left\{|h_{\mathrm{SD}}|^2 < \frac{\gamma_{\mathrm{th}}}{\rho_0}, |h_{\mathrm{SR}}|^2 < \frac{\gamma'_{\mathrm{th}}}{\rho_0}, (j-i)\,\delta E_0 \le \eta|h_{\mathrm{SR}}|^2 E_0 < (j-i+1)\,\delta E_0\right\}}_{C_{i,j}}, & i \ne 0. \end{cases} \end{aligned} \quad (11)$$

$$\begin{aligned} P_{i,N} = \Pr\{\theta = 1, E_h \ge (N-i)\,E_u\} &= \underbrace{\Pr\left\{|h_{\mathrm{SD}}|^2 \ge \frac{\gamma_{\mathrm{th}}}{\rho_0}, 2\eta|h_{\mathrm{SR}}|^2 E_0 \ge (N-i)\,\delta E_0\right\}}_{A_{i,N}} \\ &\quad + \begin{cases} \underbrace{\Pr\left\{|h_{\mathrm{SD}}|^2 < \frac{\gamma_{\mathrm{th}}}{\rho_0}, |h_{\mathrm{SR}}|^2 < \frac{\gamma'_{\mathrm{th}}}{\rho_0} + \frac{\delta}{\eta}, \eta|h_{\mathrm{SR}}|^2 E_0 \ge \varpi E_0\right\}}_{B_{i,N}}, & i = 0, \\ \underbrace{\Pr\left\{|h_{\mathrm{SD}}|^2 < \frac{\gamma_{\mathrm{th}}}{\rho_0}, |h_{\mathrm{SR}}|^2 < \frac{\gamma'_{\mathrm{th}}}{\rho_0}, \eta|h_{\mathrm{SR}}|^2 E_0 \ge (N-i)\,\delta E_0\right\}}_{C_{i,N}}, & i \ne 0. \end{cases} \end{aligned} \quad (15)$$

energy quantum E_u, with the transition probability given as

$$\begin{aligned} P_{i,i} &= \Pr\{E_h < E_u, \theta = 1 \,|E_{\rm ini} > 0\} \\ &= \underbrace{\Pr\left\{|h_{\rm SD}|^2 \geq \frac{\gamma_{\rm th}}{\rho_0}, 2\eta|h_{\rm SR}|^2 E_0 < \delta E_0\right\}}_{A_{i,i}} \\ &\quad + \underbrace{\Pr\left\{|h_{\rm SD}|^2 < \frac{\gamma_{\rm th}}{\rho_0}, |h_{\rm SR}|^2 < \frac{\gamma'_{\rm th}}{\rho_0}, \eta|h_{\rm SR}|^2 E_0 < \delta E_0\right\}}_{B_{i,i}}, \end{aligned} \tag{19}$$

where $A_{i,i}$, and $B_{i,i}$ $(1 \leq i \leq N-1)$ are respectively given by

$$A_{i,i} = \bar{F}_{|h_{\rm SD}|^2}\left(\frac{\gamma_{\rm th}}{\rho_0}\right) F_{|h_{\rm SR}|^2}\left(\frac{\delta}{2\eta}\right), \tag{20}$$

and

$$B_{i,i} = \begin{cases} F_{|h_{\rm SD}|^2}\left(\frac{\gamma_{\rm th}}{\rho_0}\right) F_{|h_{\rm SR}|^2}\left(\frac{\gamma'_{\rm th}}{\rho_0}\right), & \frac{\gamma'_{\rm th}}{\rho_0} < \frac{\delta}{\eta}, \\ F_{|h_{\rm SD}|^2}\left(\frac{\gamma_{\rm th}}{\rho_0}\right) F_{|h_{\rm SR}|^2}\left(\frac{\delta}{\eta}\right), & \frac{\gamma'_{\rm th}}{\rho_0} \geq \frac{\delta}{\eta}. \end{cases} \tag{21}$$

5) $s_N \to s_N$

The battery can keep the fully charged state as long as R stays in the non-cooperative mode without consuming any energy. Therefore, the probability of this transition can be characterized as

$$\begin{aligned} P_{N,N} &= \Pr\{\theta = 1 \,|E_{\rm ini} > 0\} = \Pr\left\{|h_{\rm SD}|^2 \geq \frac{\gamma_{\rm th}}{\rho_0}\right\} \\ &\quad + \Pr\left\{|h_{\rm SD}|^2 < \frac{\gamma_{\rm th}}{\rho_0}, |h_{\rm SR}|^2 < \frac{\gamma'_{\rm th}}{\rho_0}\right\} \\ &= \bar{F}_{|h_{\rm SD}|^2}\left(\frac{\gamma_{\rm th}}{\rho_0}\right) + F_{|h_{\rm SD}|^2}\left(\frac{\gamma_{\rm th}}{\rho_0}\right) F_{|h_{\rm SR}|^2}\left(\frac{\gamma'_{\rm th}}{\rho_0}\right). \end{aligned} \tag{22}$$

6) $s_i \to s_0 (1 \leq i \leq N)$

This case happens when R works in the cooperative mode, and thus the stored energy is used up. The corresponding transition probability can be evaluated as

$$\begin{aligned} P_{i,0} &= \Pr\left\{\theta = 1 - \frac{\gamma'_{\rm th}}{\rho_0 |h_{\rm SR}|^2} \,|E_{\rm ini} > 0\right\} \\ &= \Pr\left\{|h_{\rm SD}|^2 < \frac{\gamma_{\rm th}}{\rho_0}, |h_{\rm SR}|^2 \geq \frac{\gamma'_{\rm th}}{\rho_0}\right\} \\ &= F_{|h_{\rm SD}|^2}\left(\frac{\gamma_{\rm th}}{\rho_0}\right) \bar{F}_{|h_{\rm SR}|^2}\left(\frac{\gamma'_{\rm th}}{\rho_0}\right). \end{aligned} \tag{23}$$

7) $s_i \to s_j (1 \leq j < i \leq N)$

Since the best effort transmission policy is employed, the battery's transitions from a higher energy state to a lower non-empty energy state cannot happen, i.e., $P_{i,j} = 0\,(1 \leq j < i \leq N)$.

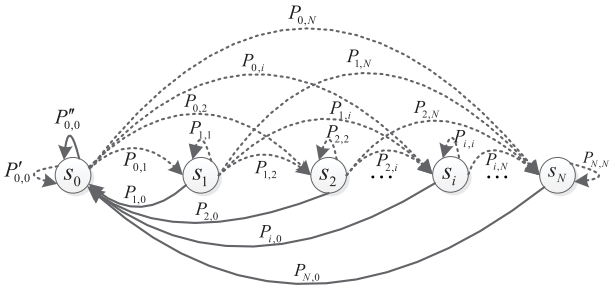

FIGURE 3. Battery state transition diagram.

According to the above analysis, the state transition diagram of the considered $(N+1)$-state MC can be constructed as Fig. 3, in which the solid lines represent that R works in the cooperative mode, and the dash lines denote that R works in the non-cooperative mode. Using the approach given in [28], the steady-state distribution of the considered MC can be calculated as[7]

$$\begin{aligned} \boldsymbol{\pi} &= (\pi_0, \pi_1, \cdots, \pi_N) \\ &= \mathbf{1}_{1\times(N+1)}\left(\mathbf{P} - \mathbf{I}_{(N+1)\times(N+1)} + \mathbf{1}_{(N+1)\times(N+1)}\right)^{-1}, \end{aligned} \tag{24}$$

where π_i $(0 \leq i \leq N)$ is steady-state probability of state s_i, $\mathbf{I}_{(N+1)\times(N+1)}$ is an $(N+1)\times(N+1)$ identity matrix, $\mathbf{1}_{(N+1)\times(N+1)}$ is an $(N+1)\times(N+1)$ matrix with all-one elements, and $\mathbf{1}_{1\times(N+1)}$ is a row vector of size $(N+1)$ with all elements equal to one.

III. OUTAGE PERFORMANCE ANALYSIS

For the target transmission block, if the achievable rate of D is less than the target rate, we say an outage happens. In this section, we analyze the outage performance of the considered system. By using the steady-state probability of the considered MC derived in the previous section, exact and asymptotic closed-form expressions of the outage probability are respectively obtained.

[7]We can also use the Sheskin algorithm adopted in [29] to calculate the steady-state probabilities of the considered MC, to avoid matrix inversion and multiplication.

$$\begin{aligned} P_{\text{out-I}} &= \sum_{i=0}^{N} \pi_i \Pr\left\{|h_{\rm SD}|^2 < \frac{\gamma_{\rm th}}{\rho_0}\right\} \Pr\{\theta = 1 \,|E_{\rm ini} = iE_u\} \\ &= \pi_0 \Pr\left\{|h_{\rm SD}|^2 < \frac{\gamma_{\rm th}}{\rho_0}\right\} \Pr\left\{|h_{\rm SR}|^2 < \frac{\gamma'_{\rm th}}{\rho_0} + \frac{\delta}{\eta}\right\} + \sum_{i=1}^{N} \pi_i \Pr\left\{|h_{\rm SD}|^2 < \frac{\gamma_{\rm th}}{\rho_0}\right\} \Pr\left\{|h_{\rm SR}|^2 < \frac{\gamma'_{\rm th}}{\rho_0}\right\} \\ &= \pi_0 F_{|h_{\rm SD}|^2}\left(\frac{\gamma_{\rm th}}{\rho_0}\right) F_{|h_{\rm SR}|^2}\left(\frac{\gamma'_{\rm th}}{\rho_0} + \frac{\delta}{\eta}\right) + (1-\pi_0) F_{|h_{\rm SD}|^2}\left(\frac{\gamma_{\rm th}}{\rho_0}\right) F_{|h_{\rm SR}|^2}\left(\frac{\gamma'_{\rm th}}{\rho_0}\right). \end{aligned} \tag{25}$$

A. EXACT OUTAGE PROBABILITY

According to our proposed AHSU strategy, the outage event for the considered system appears in the following two cases:

Case I: D feeds back an NACK, i.e., $|h_{\mathrm{SD}}|^2 < \frac{\gamma_{\mathrm{th}}}{\rho_0}$. Meanwhile, R works in the non-cooperative mode. By using the law of total probability, the outage probability $P_{\text{out-I}}$ for Case I can be directly calculated as (25), as shown at the bottom of the previous page.

Case II: D feeds back an NACK and R works in the cooperative mode, but the total received SNR at D is less than the decoding threshold γ'_{th}. The outage probability $P_{\text{out-II}}$ for this case is given by (26), as shown at the bottom of this page. The derivation of (26) and the definition of $\Xi(\cdot)$ can be found in Appendix A.

To this end, the exact outage probability with our AHSU strategy $P_{\text{out-AHSU}}$ can be obtained as a summation of $P_{\text{out-I}}$ and $P_{\text{out-II}}$.

Remark 1: For the special case with $\pi_N = 1$, the considered system reduces to the conventional incremental relaying (CIR) system where R also has constant power supply and the transmit power of R is $P_{\mathrm{R}} = \varpi P_{\mathrm{S}}$. By substituting $\boldsymbol{\pi} = (0, 0, \ldots, 1)$ into (25) and (26) and combining the derived results, the outage probability for the CIR network is given by

$$P_{\text{out-CIR}} = F_{|h_{\mathrm{SD}}|^2}\left(\frac{\gamma_{\mathrm{th}}}{\rho_0}\right) F_{|h_{\mathrm{SR}}|^2}\left(\frac{\gamma'_{\mathrm{th}}}{\rho_0}\right) + \bar{F}_{|h_{\mathrm{SR}}|^2}\left(\frac{\gamma'_{\mathrm{th}}}{\rho_0}\right) \Xi(\varpi). \tag{27}$$

B. ASYMPTOTIC OUTAGE PROBABILITY

Noting that the inverse matrix calculation is involved in the derivation of the steady-state probability $\boldsymbol{\pi}$, the complexity of calculating the exact outage probability increases as N enlarges. Further, the derived exact outage probability expression $P_{\text{out-AHSU}}$ fails to provide further insights (e.g., how do the system parameters affect the outage performance?). In this sense, we investigate the outage performance in the high SNR regime ($\rho_0 \to \infty$), which effectively eases the computation and reveals some useful insights such as the diversity order and coding gain of the considered system.

Lemma 1: The steady-state probabilities of the considered MC in the high SNR regime can be approximated as

$$\pi_0 \approx \pi_0^{\text{asy}} \triangleq \frac{1-a}{1-a+ab}, \tag{28a}$$

$$\pi_i \approx \pi_i^{\text{asy}} \triangleq \frac{ab(1-a)(1-b)}{(1-a+ab)^2}\left(\frac{b}{1-a+ab}\right)^{i-1}, \quad 1 \le i \le N-1 \tag{28b}$$

$$\pi_N \approx \pi_N^{\text{asy}} \triangleq a\left(\frac{b}{1-a+ab}\right)^{N}, \tag{28c}$$

where $a = 1 - \frac{\gamma_{\mathrm{th}}}{\rho_0 \Omega_{\mathrm{SD}}}$, and $b = e^{-\frac{\delta}{2\eta\Omega_{\mathrm{SR}}}}$.

The proof of *Lemma* 1 is given in Appendix B.

Remark 2: It is easy to check that with the increase of a or b, π_0^{asy} decreases and π_N^{asy} increases, which indicates that π_0^{asy} and π_N^{asy} are respectively a decreasing and an increasing function of ρ_0, Ω_{SD}, η, Ω_{SR} and $\gamma_{\mathrm{th}}^{-1}$. This can be explained by the following two facts: 1) When the transmit SNR ρ_0 and the direct link channel gain Ω_{SD} are larger, while the decoding threshold γ_{th} is smaller, the chance that D successfully decodes S's message via the direct link is larger, and thus, R has more opportunities to work in the non-cooperation mode (i.e., R only harvests energy without information decoding). 2) When the energy conversion efficiency η and the average channel gain Ω_{SR} are larger, R can harvest more energy each time.

After deriving the approximation of the steady-state probabilities, we are ready to obtain the asymptotic outage probability.

Corollary 1: The asymptotic outage probability with the AHSU strategy is given by

$$P_{\text{out-AHSU}}^{\text{asy}} \approx \frac{\Psi_1 + \Psi_2}{\rho_0^2}, \tag{29}$$

where

$$\Psi_1 = \frac{\gamma_{\mathrm{th}}}{\Omega_{\mathrm{SD}}}\left[\frac{\gamma_{\mathrm{th}}\left(e^{\frac{\delta}{2\eta\Omega_{\mathrm{SR}}}} - e^{-\frac{\delta}{2\eta\Omega_{\mathrm{SR}}}}\right)}{\Omega_{\mathrm{SD}}} + \frac{\gamma'_{\mathrm{th}}}{\Omega_{\mathrm{SR}}}\right], \tag{30}$$

and

$$\Psi_2 = \frac{\gamma_{\mathrm{th}}\left(2\gamma'_{\mathrm{th}} - \gamma_{\mathrm{th}}\right)}{2\Omega_{\mathrm{SD}}\Omega_{\mathrm{RD}}}\left[\frac{1}{\delta}\left(1 - e^{-\frac{\delta}{\eta\Omega_{\mathrm{SR}}}}\right) \times \left(\sum_{l=1}^{N-1}\frac{\pi_0^{\text{asy}}}{l}e^{-\frac{l\delta}{\eta\Omega_{\mathrm{SR}}}} + \sum_{i=1}^{N-1}\sum_{l=0}^{N-i-1}\frac{\pi_i^{\text{asy}}}{i+l}e^{-\frac{l\delta}{\eta\Omega_{\mathrm{SR}}}}\right) + \frac{1}{\varpi}\sum_{i=0}^{N}\pi_i^{\text{asy}}e^{-\frac{(N-i)\delta}{\eta\Omega_{\mathrm{SR}}}}\right]. \tag{31}$$

The proof of *Corollary* 1 is given in Appendix C.

$$\begin{aligned} P_{\text{out-II}} = {} & \pi_0 \sum_{l=1}^{N-1}\left[F_{|h_{\mathrm{SR}}|^2}\left(\frac{\gamma'_{\mathrm{th}}}{\rho_0} + \frac{(l+1)\delta}{\eta}\right) - F_{|h_{\mathrm{SR}}|^2}\left(\frac{\gamma'_{\mathrm{th}}}{\rho_0} + \frac{l\delta}{\eta}\right)\right]\Xi(l\delta) \\ & + \sum_{i=1}^{N-1}\sum_{l=0}^{N-i-1}\pi_i\left[F_{|h_{\mathrm{SR}}|^2}\left(\frac{\gamma'_{\mathrm{th}}}{\rho_0} + \frac{(l+1)\delta}{\eta}\right) - F_{|h_{\mathrm{SR}}|^2}\left(\frac{\gamma'_{\mathrm{th}}}{\rho_0} + \frac{l\delta}{\eta}\right)\right]\Xi((i+l)\delta) \\ & + \sum_{i=0}^{N}\pi_i\bar{F}_{|h_{\mathrm{SR}}|^2}\left(\frac{\gamma'_{\mathrm{th}}}{\rho_0} + \frac{(N-i)\delta}{\eta}\right)\Xi(\varpi). \end{aligned} \tag{26}$$

Remark 3: From (29), we know that the diversity order and coding gain of the considered system with our AHSU strategy are respectively given by $G_d = 2$ and $G_c = (\Psi_1 + \Psi_2)^{-\frac{1}{2}}$. Following a similar analysis to that in Appendix C, the asymptotic outage probability of the CIR network is given by

$$P_{\text{out-CIR}}^{\text{asy}} \approx \frac{\gamma_{\text{th}}}{\Omega_{\text{SD}}} \left(\frac{\gamma'_{\text{th}}}{\Omega_{\text{SR}}} + \frac{2\gamma'_{\text{th}} - \gamma_{\text{th}}}{2\varpi\,\Omega_{\text{RD}}} \right) (\rho_0)^{-2}. \quad (32)$$

Comparing (29) and (32), we find that the considered system with our AHSU strategy can achieve the same diversity order as that achieved in CIR network, which is a full diversity order. In our considered system, the battery size ϖE_0 and the energy conversion efficiency η have no impact on the diversity order, while they affect the coding gain of the system.

IV. NUMERICAL RESULTS

In this section, we provide numerical results to verify our theoretical analysis given in the previous section. Unless otherwise stated, the following parameters are used. The transmit power of S is $P_{\text{S}} \in [-20\text{dBm}, 30\text{dBm}]$, the target rate is $R_t = 2$ bits/sec/Hz, the energy conversion efficiency is $\eta = 0.5$, the noise power is $\sigma^2 = -70\text{dBm}$, and the distance between S $\to$ D, S $\to$ R, and R $\to$ D are set to be $d_{\text{SD}} = 10\text{m}$, $d_{\text{SR}} = 5\text{m}$, and $d_{\text{RD}} = 10\text{m}$, respectively. Similar to [30], the path gain corresponding to a distance of 1 meter is $\lambda = -20\text{dB}$, and the path loss exponent is $\nu = 3$.

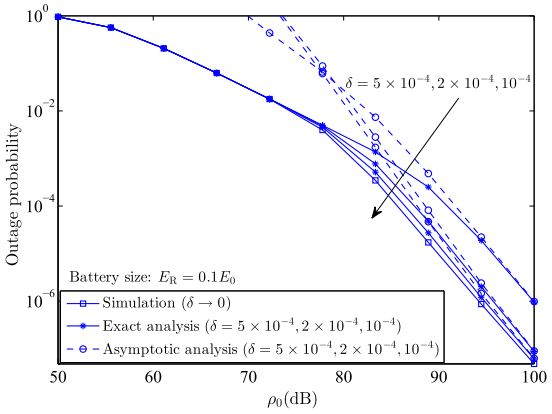

FIGURE 4. Outage performance for different energy quantum E_u (δE_0).

Fig. 4 illustrates the outage probability with the proposed AHSU strategy for different energy quantum E_u (δE_0). In addition, the simulation results for continuous battery model, i.e., $\delta \to 0$, are also given as a reference. It can be seen that the asymptotic results well agree with the exact results in the high SNR regime, which verifies the accuracy of the asymptotic analysis. We can also notice that in the medium SNR regime ($\rho_0 = 50\,\text{dB} \sim 75\,\text{dB}$), our derived analytical results using the quantization model for the battery energy almost coincide with the results of the continuous battery model. The reason is as follows. When the transmit SNR ρ_0 is not high, the battery energy keeps at a low level, and thus, effect of quantization errors (introduced by the quantization model) when quantizing high battery energy levels disappears. When the transmit SNR increases (beyond 80dB), the battery energy can reach higher levels, and thus, quantization errors when quantizing high battery energy levels start to take effect. So there is a gap between our derived analytical results and the simulation results. As δ decreases, our derived analytical results gradually approach the simulation results. This observation suggests that in order to accurately characterize the continuous battery level using the quantization model, the energy quantum E_u should be small enough.

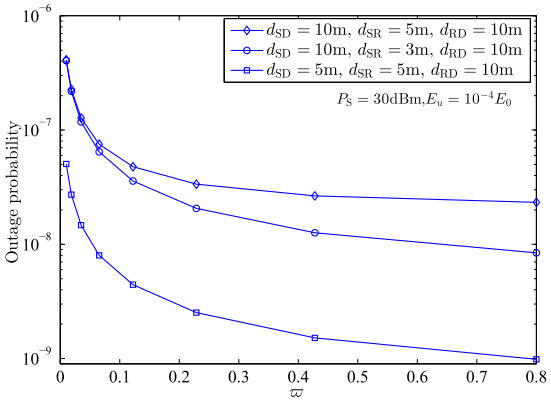

FIGURE 5. Outage performance for different battery size E_{R} (ϖE_0).

Fig. 5 examines the impact of battery capacity E_{R} (ϖE_0) on the system performance. It can be observed that the outage probability first monotonically decreases as the battery capacity increases. This can be explained by the fact that enlarging the battery capacity avoids energy overflow in the process of energy storage. Continuing to increase the battery capacity, the outage performance reaches the floor. However, the rate of approaching the floor varies for different network setups. This phenomenon suggests that different network setup requires different battery size. According to *Remark* 2, we know that when the distance of S $\to$ D and S $\to$ R are small, R not only has more chances to harvest energy, but also collects more energy each time. Thus, a large battery size is required in this case.

Fig. 6 compares the outage performance of the considered system in the following three energy management strategies: AHSU, HU and IATF. For the HU strategy, the PS ratio at the EH-based relay is set as $\theta = \max\left\{1 - \frac{\gamma'_{\text{th}}}{\rho_0 |h_{\text{SR}}|^2}, 0\right\}$. In addition, the outage performance of the direct transmission (DT) (in which there is no cooperation of the relay) and CIR network are also given as benchmarks. It is observed that the CIR network has the best outage performance, as it has constant power supply. However, the considered network with the AHSU strategy almost achieves the same outage performance as that of CIR when $\varpi = 0.01$. As ϖ increases from 0.01 to 0.1, the performance gap between AHSU and CIR enlarges. This is due to the fact that R's battery is

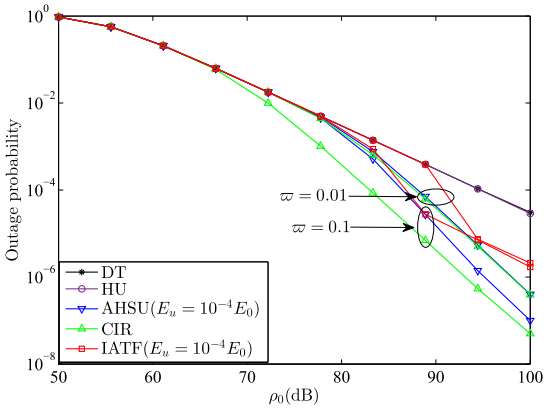

FIGURE 6. Outage performance comparison.

easy to be fully charged when the battery capacity is small. As battery capacity increases, it becomes more difficult to fully charge the battery, which results in an increasing performance gap between CIR and AHSU. We can also notice that AHSU strategy outperforms IATF and HU strategies, and IATF strategy outperforms DT strategy. It is also observed that the outage probability curves of IATF remain parallel to that of DT in the high SNR regime, which reveals that the considered system with the IATF strategy does not achieve a full diversity order. Compared to DT, the HU strategy only achieves minor performance gain, which demonstrates the importance of having a battery to accumulate energy in EH networks.

V. CONCLUSION

In this paper, we have designed a new energy harvesting and use strategy for the WPCN. Based on the 1-bit feedback from the destination, the channel estimation result for the source-to-relay link, and the relay's energy status, the proposed AHSU strategy allows the relay to harvest and use energy more efficiently. To facilitate performance analysis, a discretized MC has been applied to model the charging and discharging process of the relay's battery. We have derived the exact outage probability for the considered network. Then, a simple yet valuable expression of the asymptotic outage probability has been obtained, which illustrates that the considered network with the proposed AHSU strategy can achieve a full diversity order. Numerical results have showed that the proposed AHSU strategy outperforms the HU and IATF strategies.

APPENDIX A
DERIVATION OF EQUATION (26)

Recall that the energy level at the beginning of the target transmission block is $E_{\text{ini}} = iE_u$, and the amount of harvested energy that can be stored in the battery in the target transmission block is $\tilde{E}_h = lE_u$. When D feeds back an NACK (i.e., $|h_{\text{SD}}|^2 < \frac{\gamma_{\text{th}}}{\rho_0}$) and R works in the cooperative mode, the instantaneous SNR of the R $\to$ D link, according to the best effort transmission policy, can be written as

$$\gamma_{\text{RD}} = \frac{\left(\tilde{E}_h + E_{\text{ini}}\right)|h_{\text{RD}}|^2}{T\sigma^2/2} = \delta\,(l+i)\,\rho_0|h_{\text{RD}}|^2. \quad (33)$$

As such, the total received SNR at D after MRC is given by

$$\gamma_t = \rho_0|h_{\text{SD}}|^2 + \psi\,\rho_0|h_{\text{RD}}|^2, \quad (34)$$

where $\psi = \delta\,(l+i)$. By using the law of total probability, the outage probability for Case II is finally given by

$$P_{\text{out-II}} = \sum_{i=0}^{N}\sum_{l=0}^{N-i}\pi_i \Pr\left\{\tilde{E}_h = lE_u, \theta = 1 - \frac{\gamma'_{\text{th}}}{\rho_0|h_{\text{SR}}|^2}\,|E_{\text{ini}} = iE_u\right\} \times \underbrace{\Pr\left\{|h_{\text{SD}}|^2 < \frac{\gamma_{\text{th}}}{\rho_0}, \gamma_t < \gamma'_{\text{th}}\right\}}_{\Xi(\psi)}, \quad (35)$$

where $\Xi(\cdot)$ is defined and derived as follows

$$\begin{aligned}\Xi(x) &= \int_0^{\frac{\gamma_{\text{th}}}{\rho_0}} \Pr\left\{|h_{\text{RD}}|^2 < \frac{\gamma'_{\text{th}} - \rho_0 v}{x\rho_0}\right\} f_{|h_{\text{SD}}|^2}(v)\,dv \\ &= \frac{1}{\Omega_{\text{SD}}}\int_0^{\frac{\gamma_{\text{th}}}{\rho_0}} \left(1 - e^{-\frac{\gamma'_{\text{th}} - \rho_0 v}{x\rho_0\Omega_{\text{RD}}}}\right) e^{-\frac{v}{\Omega_{\text{SD}}}}\,dv \\ &= \begin{cases} 1 - e^{-\frac{\gamma_{\text{th}}}{\rho_0\Omega_{\text{SD}}}} - \frac{x\Omega_{\text{RD}}e^{-\frac{\gamma'_{\text{th}}}{x\rho_0\Omega_{\text{RD}}}}}{(\Omega_{\text{SD}} - x\Omega_{\text{RD}})} \\ \times\left(e^{\frac{\gamma_{\text{th}}}{\rho_0}\left(\frac{1}{x\Omega_{\text{RD}}} - \frac{1}{\Omega_{\text{SD}}}\right)} - 1\right), & \text{if } \Omega_{\text{SD}} \neq x\Omega_{\text{RD}}, \\ 1 - e^{-\frac{\gamma_{\text{th}}}{\rho_0\Omega_{\text{SD}}}} - \frac{\gamma_{\text{th}}}{\rho_0\Omega_{\text{SD}}}e^{-\frac{\gamma'_{\text{th}}}{\rho_0\Omega_{\text{SD}}}}, & \text{if } \Omega_{\text{SD}} = x\Omega_{\text{RD}}. \end{cases}\end{aligned} \quad (36)$$

To this end, we can get (26) by substituting (4), (5) and (36) into (35).

APPENDIX B
PROOF OF LEMMA 1

In the high SNR regime as $\rho_0 \to \infty$, we have $\frac{\gamma'_{\text{th}}}{\rho_0} < \frac{\delta}{\eta}$. By using this condition along with the series expansion of exponential function, the transition probability of the considered MC can be re-expressed as

$$s_0 \to s_0 : P_{0,0} = 1 - ab + o\left(\rho_0^{-1}\right) \approx 1 - ab; \quad (37a)$$

$$s_i \to s_j : P_{i,j} = a\,(1-b)\,b^{j-i} + o\left(\rho_0^{-1}\right) \approx a\,(1-b)\,b^{j-i}, \quad 0 \le i < j < N; \quad (37b)$$

$$s_i \to s_N : P_{i,N} = ab^{N-i} + o\left(\rho_0^{-1}\right) \approx ab^{N-i}, \quad 0 \le i < N; \quad (37c)$$

$$s_i \to s_i : P_{i,i} = a\,(1-b) + o\left(\rho_0^{-1}\right) \approx a\,(1-b), \quad 1 \le i \le N-1; \quad (37d)$$

$$s_N \to s_N : P_{N,N} = a + o\left(\rho_0^{-1}\right) \approx a; \quad (37e)$$

$$s_i \to s_0 : P_{i,0} = 1 - a + o\left(\rho_0^{-1}\right) \approx 1 - a, \quad 1 \le i \le N; \quad (37f)$$

$$s_i \to s_j : P_{i,j} = 0, \quad 1 \le j < i \le N, \quad (37g)$$

$$\mathbf{P}=\begin{bmatrix} 1-ab & ab\,(1-b) & \cdots & ab^{N-1}\,(1-b) & ab^{N} \\ 1-a & a\,(1-b) & \cdots & ab^{N-2}\,(1-b) & ab^{(N-1)} \\ \vdots & 0 & \ddots & \vdots & \vdots \\ \vdots & \vdots & \ddots & a\,(1-b) & ab \\ 1-a & 0 & \cdots & 0 & a \end{bmatrix}_{(N+1)\times(N+1)}. \tag{38}$$

where $o\,(x)$ denotes the higher order terms of x, and a and b are given in (28). As such, the corresponding transition probability matrix $\mathbf{P}$ can be constructed as (38), as shown at the top of this page

With some straightforward algebraic manipulations, we can solve the system of linear equations in $\boldsymbol{\pi}\mathbf{P}=\boldsymbol{\pi}$ and $\sum_{i=0}^{N}\pi_i=1$, and finally derive the steady-state probabilities shown in *Lemma* 1.

APPENDIX C
PROOF OF COROLLARY 1

By using the series expansion of exponential function, the asymptotic outage probability for Case I can be derived as

$$P_{\text{out-I}}^{\text{asy}}=\pi_0^{\text{asy}}\frac{\gamma_{\text{th}}}{\rho_0\Omega_{\text{SD}}}\left[1-e^{-\frac{\delta}{\eta\Omega_{\text{SR}}}}\left(1-\frac{\gamma_{\text{th}}'}{\rho_0\Omega_{\text{SR}}}\right)\right]+\left(1-\pi_0^{\text{asy}}\right)\frac{\gamma_{\text{th}}}{\rho_0\Omega_{\text{SD}}}\frac{\gamma_{\text{th}}'}{\rho_0\Omega_{\text{SR}}}+o\left(\rho_0^{-2}\right). \tag{39}$$

In the high SNR regime, as $1-a=\frac{\gamma_{\text{th}}}{\rho_0\Omega_{\text{SD}}}\to 0$, we have $\pi_0^{\text{asy}}=\frac{1-a}{1-a+ab}=\frac{1}{1-b+\frac{b}{1-a}}\approx\frac{1-a}{b}$. Substituting this result into (39), $P_{\text{out-I}}^{\text{asy}}$ can be approximated as $P_{\text{out-I}}^{\text{asy}}\approx\frac{\Psi_1}{\rho_0^2}+o\left(\rho_0^{-2}\right)$, where Ψ_1 is given in (30). To obtain the asymptotic outage probability for Case II, we need to first derive the asymptotic result of $\Xi\,(x)$ defined in (36). By applying the series expansion of exponential functions, $\Xi\,(x)$ can be expressed as

$$\Xi\,(x)=\frac{\gamma_{\text{th}}}{2x\rho_0^2\Omega_{\text{SD}}\Omega_{\text{RD}}}\left(2\gamma_{\text{th}}'-\gamma_{\text{th}}\right)+o\left(\rho_0^{-2}\right). \tag{40}$$

Now substituting (40) into (26), and applying the series expansion of exponential function again, the asymptotic outage probability for Case II is obtained as $P_{\text{out-II}}^{\text{asy}}\approx\frac{\Psi_2}{\rho_0^2}+o\left(\rho_0^{-2}\right)$, where Ψ_2 is given in (31). Combining $P_{\text{out-I}}^{\text{asy}}$ and $P_{\text{out-II}}^{\text{asy}}$ and ignoring higher order terms, we can get an expression of the asymptotic outage probability, as shown in (29).

REFERENCES

[1] J. G. Andrews *et al.*, "What will 5G be?" *IEEE J. Sel. Areas Commun.*, vol. 32, no. 6, pp. 1065–1082, Jun. 2014.

[2] S. Buzzi, C.-L. I, T. E. Klein, H. V. Poor, C. Yang, and A. Zappone, "A survey of energy-efficient techniques for 5G networks and challenges ahead," *IEEE J. Sel. Areas Commun.*, vol. 34, no. 4, pp. 697–709, Apr. 2016.

[3] S. Ulukus *et al.*, "Energy harvesting wireless communications: A review of recent advances," *IEEE J. Sel. Areas Commun.*, vol. 33, no. 3, pp. 360–381, Apr. 2015.

[4] X. Lu, P. Wang, D. Niyato, D. I. Kim, and Z. Han, "Wireless networks with RF energy harvesting: A contemporary survey," *IEEE Commun. Surveys Tuts.*, vol. 17, no. 2, pp. 757–789, 2nd Quart., 2015.

[5] L. R. Varshney, "Transporting information and energy simultaneously," in *Proc. IEEE Int. Symp. Inf. Theory*, Toronto, ON, Canada, Jul. 2008, pp. 1612–1616.

[6] P. Grover and A. Sahai, "Shannon meets Tesla: Wireless information and power transfer," in *Proc. IEEE Int. Symp. Inf. Theory*, Austin, TX, USA, Jun. 2010, pp. 2363–2367.

[7] R. Zhang and C. K. Ho, "MIMO broadcasting for simultaneous wireless information and power transfer," *IEEE Trans. Wireless Commun.*, vol. 12, no. 5, pp. 1989–2001, May 2013.

[8] K. Huang and V. K. N. Lau, "Enabling wireless power transfer in cellular networks: Architecture, modeling and deployment," *IEEE Trans. Wireless Commun.*, vol. 13, no. 2, pp. 902–912, Feb. 2014.

[9] X. Zhou, R. Zhang, and C. K. Ho, "Wireless information and power transfer: Architecture design and rate-energy tradeoff," *IEEE Trans. Commun.*, vol. 61, no. 11, pp. 4754–4767, Nov. 2013.

[10] D. W. K. Ng, E. S. Lo, and R. Schober, "Wireless information and power transfer: Energy efficiency optimization in OFDMA systems," *IEEE Trans. Wireless Commun.*, vol. 12, no. 12, pp. 6352–6370, Dec. 2013.

[11] L. Liu, R. Zhang, and K.-C. Chua, "Secrecy wireless information and power transfer with MISO beamforming," *IEEE Trans. Signal Process.*, vol. 62, no. 7, pp. 1850–1863, Apr. 2014.

[12] G. Zheng, Z. Ho, E. A. Jorswieck, and B. Ottersten, "Information and energy cooperation in cognitive radio networks," *IEEE Trans. Signal Process.*, vol. 62, no. 9, pp. 2290–2303, May 2014.

[13] A. A. Nasir, X. Zhou, S. Durrani, and R. A. Kennedy, "Relaying protocols for wireless energy harvesting and information processing," *IEEE Trans. Wireless Commun.*, vol. 12, no. 7, pp. 3622–3636, Jul. 2013.

[14] Z. Ding, S. M. Perlaza, I. Esnaola, and H. V. Poor, "Power allocation strategies in energy harvesting wireless cooperative networks," *IEEE Trans. Wireless Commun.*, vol. 13, no. 2, pp. 846–860, Feb. 2014.

[15] H. Chen, Y. Li, Y. Jiang, Y. Ma, and B. Vucetic, "Distributed power splitting for SWIPT in relay interference channels using game theory," *IEEE Trans. Wireless Commun.*, vol. 14, no. 1, pp. 410–420, Jan. 2015.

[16] I. Krikidis, S. Timotheou, and S. Sasaki, "RF energy transfer for cooperative networks: Data relaying or energy harvesting?" *IEEE Commun. Lett.*, vol. 16, no. 11, pp. 1772–1775, Nov. 2012.

[17] K.-H. Liu, "Selection cooperation using RF energy harvesting relays with finite energy buffer," in *Proc. IEEE Wireless Commun. Netw. Conf. (WCNC)*, Apr. 2014, pp. 2156–2161.

[18] K.-H. Liu, "Performance analysis of relay selection for cooperative relays based on wireless power transfer with finite energy storage," *IEEE Trans. Veh. Technol.*, vol. 65, no. 7, pp. 5110–5121, Jul. 2016.

[19] Y. Gu, H. Chen, Y. Li, Y. C. Liang, and B. Vucetic, "Distributed multi-relay selection in accumulate-then-forward energy harvesting relay networks," *IEEE Trans. Green Commun. Netw.*, vol. 2, no. 1, pp. 74–86, Mar. 2018.

[20] I. Krikidis, "Relay selection in wireless powered cooperative networks with energy storage," *IEEE J. Sel. Area Commun.*, vol. 33, no. 12, pp. 2596–2610, Dec. 2015.

[21] Z. Zhou, M. Peng, Z. Zhao, W. Wang, and R. S. Blum, "Wireless-powered cooperative communications: power-splitting relaying with energy accumulation," *IEEE J. Sel. Areas Commun.*, vol. 34, no. 4, pp. 969–982, Apr. 2016.

[22] Z. Li, H. Chen, Y. Li, and B. Vucetic, "Incremental accumulate-then-forward relaying in wireless energy harvesting cooperative networks," in *Proc. IEEE GLOBECOM*, Dec. 2016, pp. 1–6.

[23] H. Lee, C. Song, S.-H. Choi, and I. Lee, "Outage probability analysis and power splitter designs for SWIPT relaying systems with direct link," *IEEE Commun. Lett.*, vol. 21, no. 3, pp. 648–651, Mar. 2017.

[24] N. T. Do, D. B. da Costa, T. Q. Duong, V. N. Q. Bao, and B. An, "Exploiting direct links in multiuser multirelay SWIPT cooperative networks with opportunistic scheduling," *IEEE Trans. Wireless Commun.*, vol. 16, no. 8, pp. 5410–5427, Aug. 2017.
[25] Z. Wen, W. Guo, N. C. Beaulieu, X. Liu, and W. Xu, "Performance of SWIPT for AF MIMO relay systems with direct link," *IEEE Commun. Lett.*, vol. 22, no. 2, pp. 340–343, Feb. 2018.
[26] J. N. Laneman, D. N. C. Tse, and G. W. Wornell, "Cooperative diversity in wireless networks: Efficient protocols and outage behavior," *IEEE Trans. Inf. Theory*, vol. 50, no. 12, pp. 3062–3080, Dec. 2004.
[27] A. Goldsmith, *Wireless Communications*. Cambridge, U.K.: Cambridge Univ. Press, 2005.
[28] I. Krikidis, T. Charalambous, and J. S. Thompson, "Buffer-aided relay selection for cooperative diversity systems without delay constraints," *IEEE Trans. Wireless Commun.*, vol. 11, no. 5, pp. 1957–1967, May 2012.
[29] A. H. Sakr and E. Hossain, "Analysis of K-tier uplink cellular networks with ambient RF energy harvesting," *IEEE J. Sel. Areas Commun.*, vol. 33, no. 10, pp. 2226–2238, Oct. 2015.
[30] S. Lee and R. Zhang, "Distributed wireless power transfer with energy feedback," *IEEE Trans. Signal Process.*, vol. 65, no. 7, pp. 1685–1699, Apr. 2017.

GUOXIN LI is currently pursuing the Ph.D. degree with the University of Alberta, Edmonton, AB, Canada. His research interests include non-orthogonal multiple access, cooperative communications, and wireless power transfer.

HAI JIANG (SM'15) received the B.Sc. and M.Sc. degrees in electronics engineering from Peking University, Beijing, China, in 1995 and 1998, respectively, and the Ph.D. degree in electrical engineering from the University of Waterloo, Waterloo, ON, Canada, in 2006. He is currently a Professor with the Department of Electrical and Computer Engineering, University of Alberta, Canada. His research interests include radio resource management, cognitive radio networking, and cooperative communications.